# Transformed Dissipation in Superconducting Quantum Circuits

Matthew Neeley, M. Ansmann, Radoslaw C. Bialczak, M. Hofheinz, N. Katz,
Erik Lucero, A. O'Connell, H. Wang, A. N. Cleland, and John M. Martinis*
*Department of Physics, University of California at Santa Barbara, Broida Hall, Santa Barbara, CA 93106*
(Dated: January 18, 2008)

Superconducting quantum circuits must be designed carefully to avoid dissipation from coupling to external control circuitry. Here we demonstrate a simple method to calculate this dissipation, based on classical impedance transformations. The method agrees quantitatively with measurements of the lifetime of a Josephson phase qubit coupled to a tunable impedance transformer. Higher-order corrections are calculated, but found not to limit the qubit lifetime. Such tunable dissipation may be useful in superconducting quantum circuits, for example in speeding up qubit reset.

PACS numbers: 03.65.Yz, 03.67.Lx, 85.25.Cp
Keywords: Josephson Junction, Quantum Computing, Decoherence, Impedance Transformer

The quantum behavior of superconducting circuits has been demonstrated by numerous experiments [1–5], and their promise as quantum information processors [6, 7] is well-established. These devices must be carefully engineered to protect their quantum states from environmental noise, particularly that from control circuitry to which the qubits are permanently wired. Environmental dissipation can generally be described by spin-boson models [8, 9] or—more practically—computed as being proportional to the real part of the admittance $Y(\omega)$, the classical response of the circuit [10].

In this letter we present a simple but powerful method to calculate the dissipation from external circuitry in a quantum circuit, such as a superconducting qubit. The predictions of this method show quantitative agreement with measurements of $T_1$ for a qubit coupled to a tunable impedance transformer. While variable $T_1$ lifetimes have been observed in superconducting circuits before [11], we have for the first time measured the actual impedance transformation of the coupler as well as the qubit lifetime, and shown that they agree according to the simple theory. This method allows one to calculate quantum noise effects using rules of thumb familiar from analog electronics. Being able to make such calculations is particularly important in designing new quantum circuits, allowing design alternatives to be evaluated and compared quickly.

A superconducting qubit is generally coupled to control circuitry via a dissipationless element, typically a capacitor or a mutual inductance. As shown schematically in Fig. 1, the external circuitry is characterized by its admittance $Y_1(\omega)$ (often $1/(50\,\Omega)$ from a transmission line) and the coupler transforms this into an effective admittance $Y_2(\omega)$ seen by the qubit. From the fluctuation-dissipation theorem, one finds that the real part of the effective admittance seen at the output of the coupler is

$$\mathrm{Re}\, Y_2(\omega) = |dI_2/dI_1|^2\, \mathrm{Re}\, Y_1(\omega), \qquad (1)$$

where $I_1$ is a current source applied at the input port, and $I_2$ is the resulting current that appears across the shorted output port (see Fig. 1b). This admittance leads to a qubit lifetime that is approximately equal to the classical decay time $T_1 \approx C/\mathrm{Re}\, Y_2(\omega_{10})$, where $\omega_{10}$ is the qubit transition frequency, and $C$ is the qubit capacitance [10]. Thus, given an environment $Y_1(\omega)$, the current transfer function $I_2(I_1)$ completely determines the dissipation seen by the qubit through the coupler. This simple result holds not only for capacitors and inductors, but also for more complicated nonlinear dissipationless couplers.

To test this idea, we measured the lifetime of a flux-biased Josephson phase qubit as a function of the current bias through a 3-junction measurement SQUID [12]. The layout and schematic of the phase qubit and measurement SQUID is shown in Fig. 2. The operation of this device has been described previously [13], and we repeat here only the relevant details. The qubit frequency is tunable over a range of several GHz by applying magnetic flux to the qubit loop. The qubit state is measured

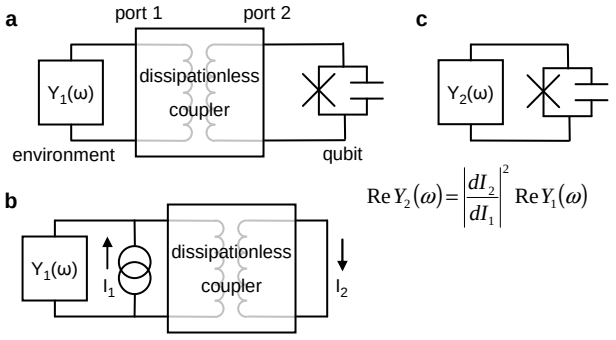


FIG. 1: Impedance transformation by a 2-port dissipationless coupler. (**a**) Qubit is connected through a dissipationless coupler to environment, described by admittance $Y_1(\omega)$ of the external circuitry. (**b**) The transfer function of the coupler relates current source $I_1$ across the input port to current $I_2$ across the shorted output. (**c**) The effective dissipation seen by the qubit at port 2 is transformed by the squared derivative of the transfer function.

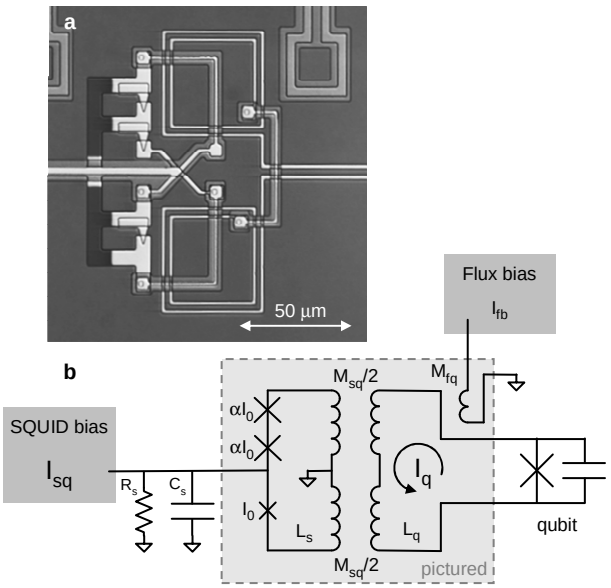


FIG. 2: Micrograph (**a**) and schematic (**b**) of the phase qubit and SQUID. The overlap of the qubit and SQUID loops increases their mutual inductance $M_{sq}$, while their gradiometric layout reduces their sensitivity to external flux. The flux bias coil couples to the qubit to tune its frequency, but has negligible mutual inductance with the SQUID. The shunt resistor $R_s$ reduces quasiparticle generation in the SQUID when it switches [14]. The qubit sees $R_s$ transformed by coupling through the SQUID. For the tested device, qubit capacitance and critical current are 1 pF and 2 $\mu$A. In addition, we have $I_0 = 2\,\mu$A, $\alpha = 1.5$, $L_s = 300$ pH, $L_q = 720$ pH, $M_{sq} = 70$ pH, $M_{fq} = 2$ pH, $R_s = 30\,\Omega$ and $C_s = 1$ pF.

by selectively tunneling the qubit $|1\rangle$ state out of the cubic well of the phase qubit potential. The tunneled $|1\rangle$ and non-tunneled $|0\rangle$ states produce different amounts of magnetic flux in the qubit loop, the difference being about one flux quantum $\Phi_0$. The critical current of the measurement SQUID is sensitive to this difference in flux, allowing us to discriminate between the two qubit states by ramping the SQUID bias and measuring the current when the SQUID switches into the voltage state.

This sensitivity to qubit flux is only necessary during measurement, and is in fact detrimental during qubit operation. If the SQUID is sensitive to flux from the qubit, then the qubit is also sensitive to flux from the SQUID; noise and dissipation in the SQUID circuit—in particular from the shunt resistance $R_s$—will decohere the qubit state. We would like to be able to modulate the SQUID's flux sensitivity, turning off the coupling during qubit operation, and turning it on only for measurement. The three-junction design makes this possible.

When bias current $I_1 = I_{sq}$ is applied to the SQUID, it divides into the upper and lower branches of the loop. The lower branch has a single Josephson junction with critical current $I_0$, whereas the upper branch has two larger Josephson junctions each with critical current $\alpha I_0$. The total current is $I_{sq} = I_U + I_L = \alpha I_0 \sin(\delta/2) + I_0 \sin(\delta)$, where $\delta$ is the superconducting phase difference across the loop. The circulating current in the loop is $I_{circ} = I_U - I_L = \alpha I_0 \sin(\delta/2) - I_0 \sin(\delta)$. This circulating current couples via a fixed mutual inductance $M_{sq}/2$ in each branch to the qubit loop, causing current $I_2 = I_q = (M_{sq}/2L_q)I_{circ}$ to flow. The derivative of the transfer function between SQUID bias current and qubit loop current is thus

$$\frac{dI_q}{dI_{sq}} = \frac{dI_q/d\delta}{dI_{sq}/d\delta} = \frac{M_{sq}}{2L_q}\frac{(\alpha/2)\cos(\delta/2) - \cos(\delta)}{(\alpha/2)\cos(\delta/2) + \cos(\delta)}. \quad (2)$$

For the case $\alpha = 2$ and at zero bias $I_{sq} = 0$, one has $\delta = 0$ and the transfer function is flat, $dI_q/dI_{sq} = 0$. With the Josephson inductances balanced in the upper and lower branches, the current flows symmetrically and fluctuations in the bias current induce no qubit current. The SQUID and qubit are decoupled, and this "insensitive point" is where the SQUID will be biased during qubit operation. Away from the insensitive point, the inductances become unbalanced and the transfer function has nonzero slope, so that SQUID and qubit are again coupled. To measure the qubit, we ramp $I_{sq}$ toward the critical current, turning the coupling on and allowing the SQUID to discriminate between the tunneled and non-tunneled qubit states.

The junction area ratio $\alpha$ determines the number and location of the insensitive points, as shown in Fig. 3. For $\alpha = 2$ there is one such point at $I_{sq} = 0$, for $\alpha < 2$ there are two points at non-zero biases, and for $\alpha > 2$ no insensitive point exists. Because of unavoidable variations in junction size during fabrication, we typically design for $\alpha \approx 1.7$ to ensure that an insensitive point will exist, yet not be too close to the critical current of the SQUID.

The tunability of the phase qubit with flux allows us to measure the transfer function of the SQUID. We first set $I_{sq} = 0$ and find the qubit resonance frequency with spectroscopy [12]. When the SQUID bias $I_{sq}$ is set to a new value, the circulating current in the SQUID produces an offset flux $\Delta\Phi_{sq} = L_q I_q$ in the qubit, shifting its frequency. We then adjust the flux bias $\Delta\Phi_{fb} = M_{fq} I_{fb}$ to bring the qubit frequency back to its original value. For the qubit frequency to be unchanged, these two fluxes must cancel, and we have $I_q = -(M_{fq}/L_q)I_{fb}$. By repeating this procedure for a range of values of SQUID bias, we build up a measurement of the transfer function $I_q(I_{sq})$, as shown in Fig. 4a. An alternative method is to hold constant the $|0\rangle$-state tunneling rate instead of the resonance frequency, but we found that the resonance frequency was a more sensitive probe of the qubit current $I_q$ and more immune to systematic errors.

Next we measure $T_1$ as a function of SQUID bias by applying a $\pi$-pulse to the qubit and measuring the decay

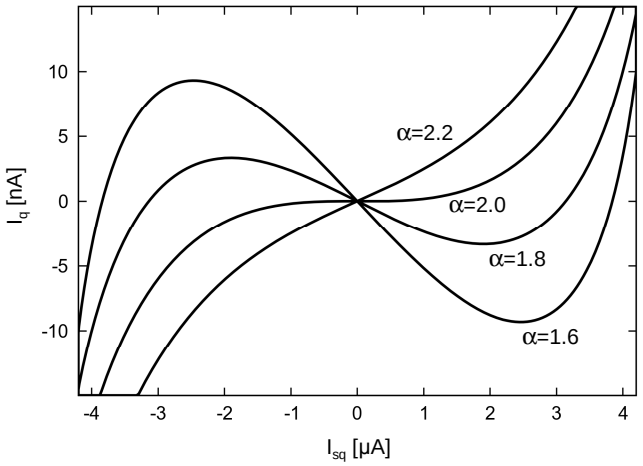


FIG. 3: Theoretical transfer function of the 3-junction SQUID. The plot shows the induced qubit current $I_q$ versus SQUID bias current $I_{sq}$, for four values of the junction size ratio $\alpha$, with device parameters as for Fig. 2. At points where $dI_q/dI_{sq} = 0$, the qubit will be insensitive to noise and dissipation from the SQUID. The design value of $\alpha = 1.7$ ensures the existence of an insensitive point that is not too close to the critical current of the SQUID.

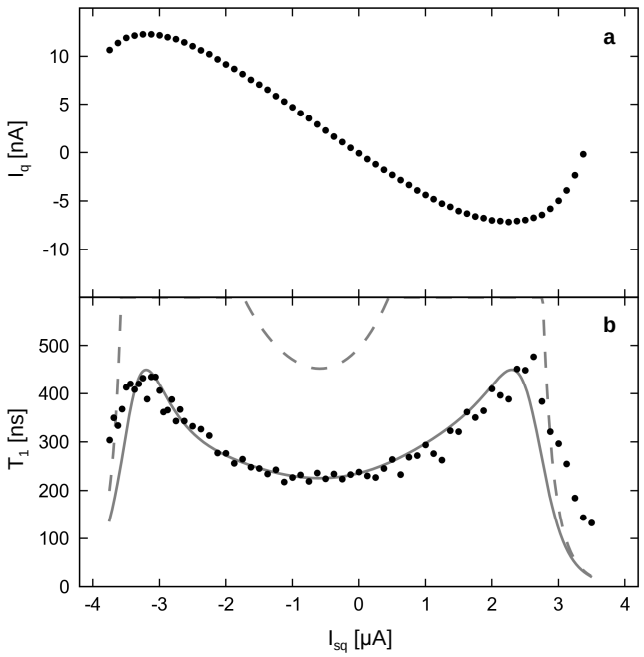


FIG. 4: Measured SQUID transfer function and its effect on qubit lifetime. (**a**) Qubit current $I_q$ versus SQUID bias $I_{sq}$, measured as described in the text. Outside the range shown, the SQUID switches prematurely, preventing reliable qubit operation. (**b**) Measured qubit lifetime $T_1$ (dots) along with theoretical curves. The dashed line is the prediction from the transfer function alone, while the solid line adds to this a constant dissipation corresponding to a lifetime of 450 ns. Best fit is for $R_s = 11\ \Omega$.

of the $|1\rangle$-state probability with time. As in the measurement of the transfer function, a flux offset is applied at each SQUID bias to keep the qubit frequency constant, removing any frequency dependence of the dissipation. Figure 4b shows the measured $T_1$ data along with predictions from the impedance-transformer model using the measured transfer function. The lifetime $T_1$ varies with SQUID bias as expected, increasing as the transfer function flattens and reaching its maxima at the insensitive points $dI_q/dI_{sq} = 0$. Beyond these biases, the transfer function has a large derivative and $T_1$ drops sharply. To fit the data, we had to add a parallel dissipation channel, independent of SQUID bias, that limits the qubit lifetime to the maximum observed value 450 ns. This lifetime is consistent with dielectric loss due to the a-Si:H dielectric of the device [15]. Using the measured slope $dI_q/dI_{sq}$, we find best agreement with shunt resistance $R_s = 11\,\Omega$ transformed by the SQUID.

The device used in this experiment has a slightly lower area ratio $\alpha$ than designed, which moves the insensitive points further away from $I_{sq} = 0$ and toward the SQUID critical current. The effect of the SQUID bias on $T_1$ is more pronounced and prevents operation very far past the extrema since the SQUID begins to switch to the voltage state.

While the agreement between theory and experiment is encouraging, there are two simplifying assumptions in the impedance transformation model that merit discussion. First, the model assumes that the coupling element is a purely inductive circuit, which has a frequency-independent transfer function. In the actual circuit, the SQUID capacitance leads to frequency-dependent effects that drastically alter the transfer function near the self-resonant frequency of the SQUID. In our device the SQUID self-resonance frequency is $\sim 15$ GHz, well above the qubit frequency of 6.75 GHz. Numerical calculations have shown that at 6.75 GHz, the SQUID capacitance simply increases the transfer function $|dI_2/dI_1|^2$ by a factor of $\sim 2$. In the circuit, the resistance from the $30\,\Omega$ shunt resistor in parallel with the $50\,\Omega$ bias line is effectively modified by this effect to give an effective shunt resistance of $(30\,\Omega||50\,\Omega)/2 \approx 9\,\Omega$. This agrees well with the best fit value of the shunt resistance $11\,\Omega$.

Secondly, the simple transformer theory predicts a diverging impedance $1/\mathrm{Re}\,Y_2$ at the extrema of the current transfer function, where $dI_q/dI_{sq} = 0$. In the experiment, we expect divergences to be rounded off by higher-order processes. The second-order effect can be calculated straightforwardly as follows: the shunt resistor $R_s$ produces a quantum noise current [16, 17] with a one-sided spectral density given in the limit $T \to 0$ by

$$S_{I_1}(f) = \begin{cases} \frac{2hf}{R_s}, & f > 0 \\ 0, & f < 0 \end{cases}, \qquad (3)$$

where $h$ is Planck's constant. The (complex) noise current $I_1(t)$ produced by this resistor is transformed by the coupler to a noise current at port 2 with Taylor expansion $I_2(t) = \text{const.} + (dI_2/dI_1)I_1(t) + (d^2I_2/dI_1^2)I_1(t)^2/2$. We calculate the spectral density of this transformed current by inserting the Fourier transform of $I_1(t)$, assuming random phases of all the frequency components. This gives for the transformed spectral density

$$S_{I_2}(f) = \left|\frac{dI_2}{dI_1}\right|^2 S_{I_1}(f) + \frac{1}{2!}\left|\frac{d^2I_2}{dI_1^2}\right|^2 \int_0^f df' S_{I_1}(f') S_{I_1}(f-f'). \quad (4)$$

The first term in this spectral density corresponds to the simple linear impedance transformation model discussed previously. The second term corresponds to dissipation due to (nonlinear) downconversion, in which the photon from port 2 at frequency $f$ is converted to two photons at frequencies $f'$ and $f''$ that are absorbed by the environment at port 1, where $f' + f'' = f$. The second-order process will dominate at the extrema of the transfer function where $dI_2/dI_1 = 0$, and lead to a finite lifetime.

The transformed spectral density may be evaluated for the spectral density of a resistor in Eq. (3), giving

$$\mathrm{Re}\, Y_2 = \frac{S_{I_2}(f)}{2hf} = \frac{1}{R_s}\left(\left|\frac{dI_2}{dI_1}\right|^2 + \frac{1}{6}\left|\frac{d^2I_2}{dI_1^2}\right|^2 \frac{hf^2}{R_s}\right). \quad (5)$$

This calculation can be extended to arbitrary order by keeping terms in the Taylor expansion of the transfer function. For a resistor the integrals can be evaluated exactly yielding

$$\mathrm{Re}\, Y_2 = \frac{1}{R_s}\sum_{k=1}^{\infty} \frac{1}{k!(2k-1)!}\left|\frac{d^kI_2}{dI_1^k}\right|^2 \left(\frac{2hf^2}{R_s}\right)^{k-1}. \quad (6)$$

The predicted lifetime due to the second-order process is $\sim 100\,\mu$s, far from the limiting value of the lifetime observed in our experiment. Thus, even accounting for second-order noise processes, we find that the SQUID is completely decoupled, as desired. Another loss mechanism, most likely dielectric loss, limits the lifetime to the observed 450 ns.

A tunable dissipation source could be a useful element in a quantum information processing device. One important requirement for a quantum computer is the ability to initialize the qubits to a fiducial input state [7]. In present devices, this is accomplished simply by waiting for the qubit to relax into the ground state $|0\rangle$. But as qubit lifetimes are extended, such waiting will decrease the experimental repetition rate. A tunable dissipation source could be used to speed up the relaxation during reset without affecting the qubit during operation. Even taking into account second-order noise processes, the off/on ratio of the tunable dissipation in the present device is several orders of magnitude, indicating that reset could be greatly accelerated even while minimizing the effects on the qubit during computation.

In conclusion, we have directly measured in a Josephson phase qubit the current transfer function of a tunable 3-junction SQUID and its transformed dissipation. The variation in qubit lifetime as a function of SQUID bias was analyzed with a simple model based on the classical impedance transformation from the measured SQUID-qubit transfer function. The dissipation predicted by this model agrees quantitatively with measurements for this non-linear coupling element. As more sophisticated quantum circuits are developed—for example in implementing tunable coupling—having a simple method to calculate environmental dissipation will become increasingly important.

Devices were made at the UCSB and Cornell Nanofabrication Facilities, a part of the NSF-funded National Nanotechnology Infrastructure Network. This work was supported by ARDA under grant W911NF-04-1-0204 and NSF under grant CCF-0507227.

* Electronic address: martinis@physics.ucsb.edu


[1] M. Sillanpaa, J. I. Park and R. W. Simmonds, Nature **449**, 438–442 (2007).
[2] J. Majer *et al.*, Nature **449**, 443–447 (2007).
[3] J. H. Plantenberg, P. C. de Groot, C. J. P. M. Harmans and J. E. Mooij, Nature **447**, 836–839 (2007).
[4] A. O. Niskanen, K. Harrabi, F. Yoshihara, Y. Nakamura, S. Lloyd and J. S. Tsai, Science **316**, 723–726 (2007).
[5] M. Steffen *et al.*, Science **313**, 1423–1425 (2006).
[6] M. A. Nielsen and I. L. Chuang, *Quantum Computation and Quantum Information* (Cambridge Univ. Press, 2000).
[7] D. P. DiVincenzo, Fortschr. d. Phys. **48**, 771–783 (2000).
[8] Y. Makhlin, G. Schön and A. Schnirman, Rev. Mod. Phys. **73**, 357 (2001).
[9] C. H. van der Wal, F. K. Wilhelm, C. J. P. M. Harmans and J. E. Mooij, Euro. Phys. J. B **31**, 111–124 (2003).
[10] D. Esteve, M. H. Devoret and J. M. Martinis, Phys. Rev. B **34**, 158 (1986).
[11] F. Yoshihara, K. Harrabi, A. O. Niskanen, Y. Nakamura and J. S. Tsai, Phys. Rev. Lett. **97**, 167001 (2006).
[12] R. W. Simmonds, K. M. Lang, D. A. Hite, S. Nam, D. P. Pappas and J. M. Martinis, Phys. Rev. Lett. **93**, 077003 (2004).
[13] M. Steffen *et al.*, Phys. Rev. Lett. **97**, 050502 (2006).
[14] K. M. Lang, S. Nam, J. Aumentado, C. Urbina and J. M. Martinis, IEEE Trans. on App. Supercond. **13**, 989–993 (2003).
[15] J. M. Martinis *et al.*, Phys. Rev. Lett. **95**, 210503 (2005).
[16] R. J. Schoelkopf, A. A. Clerk, S. M. Girvin, K. W. Lehnert and M. H. Devoret, Proc. of SPIE **5115**, 356–376 (2003).
[17] J. M. Martinis, S. Nam, J. Aumentado, K. M. Lang and C. Urbina, Phys. Rev. B **67**, 094510 (2003).